TISSUE ENGINEERING
Volume 12, Number 8, 2006
© Mary Ann Liebert, Inc.

Improved Hepatocyte Excretory Function by Immediate Presentation of Polarity Cues

SUSANNE NG,[1,2] RONGBIN HAN,[1,2] SHI CHANG, M.D.,[3] JUN NI,[1,2] WALTER HUNZIKER, Ph.D.,[3,4] ANDREW BORIS GORYACHEV, Ph.D.,[5,6] SIM HENG ONG, Ph.D.,[7] and HANRY YU, Ph.D.[1–3]

ABSTRACT

Liver tissue constructs with excretory function are crucial to developing realistic hepatocyte models for engineering effective bioartificial liver-assisted devices and for modeling the *in vivo* tissue. Current hepatocyte *in vitro* models suffer from limited or inefficient hepatocyte repolarization, which results in poor removal of xenobiotics and other waste products from the cells. We hypothesized that the temporal and spatial presentation of the cell matrix and cell-cell contacts as polarity cues would be important to define the axis of polarization to improve the excretory function of hepatocytes. The spatial presentation of polarity cues can be best achieved with sandwich configuration. We improve the temporal presentation of polarity cues by introducing the collagen overlay immediately in synchrony with cell-cell contacts instead of after 24 h in conventional sandwich culture. We demonstrate that the immediate presentation of the collagen matrix overlay enhances the formation of apicobasolateral domains, tight junctions, and the recovery of the functional activity of 2 canalicular transporters, the multidrug resistance–associated protein (Mrp2) and P-glycoprotein (P-gp) at 48 h of culture, and enhances the albumin secretion, urea production, and 7-ethoxyresorufin-O-deethylation cytochrome P450 activities of hepatocytes over 14 days of culture as compared to the 24-h overlay controls. The improvement in the excretory function of hepatocytes for the removal of waste products deleterious to cells may improve the functional maintenance and the *in vivo* fidelity of tissue-engineered liver constructs.

INTRODUCTION

ACUTE LIVER FAILURE is a rapidly progressive disorder associated with a substantial mortality rate.[1] In acute liver failure, massive necrosis of hepatocytes destroys critical metabolic, synthetic, and elimination functions of the liver. Orthotopic liver transplantation, the standard treatment for liver failure, is limited by a persistent donor shortage.[2] The tissue engineering of liver constructs may alleviate the crisis by providing temporary liver support in the form of bioartificial liver-assisted devices, potential implantable cellular constructs, and *in vitro* models for studying the pathophysiology of liver diseases and for developing less hepatotoxic drugs (hepatotoxicity is one of the leading causes of acute liver failure).[3]

Primary hepatocytes are the most common cellular component in current engineered therapies; however, primary hepatocytes lose their hepatic polarity upon isolation and

[1]Institute of Bioengineering and Nanotechnology, A*STAR, Singapore.
[2]NUS Graduate Programme in Bioengineering, NUS Graduate School for Integrative Sciences and Engineering, National University of Singapore, Singapore.
[3]Department of Physiology, National University of Singapore, Singapore.
[4]Institute of Molecular and Cell Biology, A*STAR, Singapore.
[5]Bioinformatics Institute, A*STAR, Singapore.
[6]Division of Bioengineering, National University of Singapore, Singapore.
[7]Department of Electrical and Computer Engineering, National University of Singapore, Singapore.

rapidly decline in liver-specific functions over culture time.[2] A variety of culture configurations, which recapitulate various features of the hepatocyte microenvironment *in vivo*, have improved their functional maintenance *in vitro*. These include spheroids,[4,5] sandwich cultures,[6,7] and co-cultures[8] in 3-dimensional (3D) natural or synthetic matrices.[9,10] Current culture configurations invariably suffer from limited or inefficient hepatocyte repolarization,[11] which results in poorer removal of xenobiotics and other waste products from the cells.[12] In the liver, the efficiency of passive diffusion of xenobiotics across the canalicular membrane is poor; instead, several active transporters exist on this membrane that efflux a variety of endogenous and exogenous materials from the cell into the bile canaliculus. Two canalicular active transporters have been demonstrated to contribute to the efflux of xenobiotics, the multidrug resistance–associated protein (Mrp2) and P-glycoprotein (P-gp).[13] Mrp2 is a major transporter of bilirubin, glucuronide and glutathione conjugates, and other organic anions from liver into bile,[13,14] while P-gp facilitates the excretion of exogenous organic cations and a wide variety of drugs, such as alkaloids and anthracyclines, into bile.[13,15] Improved hepatocyte repolarization may improve the functional activity of these canalicular transporters, which, in turn, facilitate the efficient excretion of waste products into a bile canalicular network that is structurally separate from the cells.

A systemic approach to characterize factors that may stimulate hepatocyte repolarization may be derived from other epithelial cell models, such as Madin-Darby canine kidney (MDCK) and mammary gland epithelial cells. Studies from these columnar epithelial cells have long highlighted the importance of cell-matrix and cell-cell interactions as external polarity cues.[16,17] In a review on new perspectives in generating epithelial cell polarity, Yeaman *et al*. proposed a model in which cell-matrix and cell-cell adhesion generate membrane asymmetry which orientates the apicobasal axis of polarity relative to the external cues.[18] On the basis of the above model, the success of the sandwich culture in partially promoting hepatocyte repolarization (in which cells are sandwiched with 2 layers of matrices to mimic the *in vivo* space of Disse) may be due to the spatial presentation of cell-matrix and cell-cell contacts as 2 polarity cues to define the axis of polarization. We hypothesized that the temporal presentation of the 2 polarity cues would also be important to define the axis of polarization. To test the hypothesis, we sought to improve the temporal presentation of polarity cues by immediately presenting the collagen overlay in synchrony with cell-cell contacts instead of after 24 h, as is done in the conventional sandwich culture. For this purpose, gelled collagen-coated inserts were developed to immediately sandwich the cells without interfering with the formation of cell-cell contacts. The enhancement of hepatocyte repolarization may improve the excretion of waste products deleterious to cells in tissue-engineered liver constructs and may provide a better model for investigating the hepatobiliary toxicity of xenobiotics.

MATERIALS AND METHODS

All reagents were purchased from Sigma-Aldrich (St. Louis, MO) unless otherwise stated.

Collagen coating and characterization

A total of 120 μL of neutralized 1.5 mg/mL type I bovine dermal collagen (8 mL collagen, 1 mL 0.1 M sodium hydroxide, 1 mL 10×phosphate-buffered saline [PBS], 6 mL 1×PBS) from Vitrogen, Angiotech BioMaterials Corp. (Palo Alto, CA), were spotted onto hydrophobic Petri dishes and 12-mm cellulose paper inserts (Millipore Corp., Billerica, MA). Glass coverslips were placed on the droplets for 20 min before they were transferred into a 37°C incubator overnight so that collagen gelation would occur. Backscattering confocal microscopy (Fluoview 300, Olympus, Melville, NY) was used to measure the thickness of the collagen coating by the use of optical sectioning with a z resolution of 0.5 μm to obtain a 3D reconstruction of the collagen-coated inserts.

Fluorescein isothiocyanate-dextran diffusivity measurements

Measurement of the diffusivity of fluorescein isothiocyanate (FITC)–conjugated dextrans of 9.5 kDa, 70 kDa, and 150 kDa through the collagen-coated inserts was based on a donor-receptor compartment model reported elsewhere.[19] The collagen-coated inserts were clamped between the receptor and donor compartments by using Minusheet carriers (Minucells and Minutissue Vertriebs GmbH, Bad Abbach, Germany). Donor compartments were filled with 80 μL of 0.2 wt % FITC-dextran in 1×PBS, while receptor compartments were filled with 200 μL of 1×PBS. A total of 80 μL of samples were taken from the receptor compartment each hour and replaced with equal volume of fresh PBS. Both donor and receiver compartments were gently agitated on a shaker throughout the experiments. The concentrations of FITC-dextran were measured at 490 nm (excitation)/525 nm (emission) against FITC-dextran standards using a microplate reader (Tecan Trading AG, Männedorf, Switzerland).

Hepatocyte isolation and culture

Hepatocytes were harvested from male Wistar rats weighing 250–300 g by a 2-step *in situ* collagenase perfusion method.[20] Routinely, 200–300 million cells were isolated with viability above 90% as determined by Trypan Blue exclusion assay. Freshly isolated rat hepatocytes were seeded on the collagen-coated inserts and coverslips based

on 3,118 cells/mm^2 (0.25 million per 8.5-mm diameter attachment area) for 1 h. Hepatocytes in the immediate overlay sandwich configuration were then immediately overlaid with collagen-coated inserts that were secured using the O-rings on the Minusheet carriers. Hepatocytes in the conventional sandwich culture were overlaid with ungelled collagen after 24-h culture, and gelation was allowed to occur at 37°C for 2.5 h before fresh culture medium was added. Hepatocytes were cultured with Hepatozyme SFM (Gibco Laboratories, Carlsbad, California), supplemented with 39 ng/mL dexamethasone, 100 U/mL penicillin, and 100 μg/mL streptomycin.

Immunofluorescence microscopy

Primary anti-CD147 mouse monoclonal antibody was purchased from Serotec, Inc. (Raleigh, NC). Primary anti-MRP2 rabbit polyclonal antibody was purchased from Sigma-Aldrich. Primary anti-ZO-1 rabbit polyclonal antibody was purchased from Zymed Laboratories (San Francisco, CA). Secondary Pacific Blue goat anti–rabbit and Alexa Fluor 635 goat anti–mouse were purchased from Molecular Probes (Eugene, OR). The 3.7% paraformaldehyde-fixed samples were blocked in 10% fetal calf serum at room temperature for 1 h. Samples were incubated with the primary antibodies (1:10) overnight at 4°C before being rinsed with 1×PBS 3 times, each rinse lasting 5 min. Samples were then incubated with the secondary antibodies at room temperature for 1 h and rinsed with 1×PBS before being mounted with FluorSave (Calbiochem, San Diego, CA). The samples were viewed with a confocal microscope (Fluoview 500, Olympus) using a 60× water lens.

Quantification of ZO-1 from cell boundary

The spread of ZO-1 from the cell boundary was quantified by implementing an image processing algorithm. The gray component of the images of CD147-stained cells (Fig. 1A) was first thresholded and the subsequent binary image subjected to a thinning algorithm to give 1-pixel-thick cell boundaries (image I_1; Fig. 1C). The green component of the images of ZO-1–stained cells (Fig. 1B) was thresholded to give image I_2 (Fig. 1D), in which the white pixels indicate the regions that contain a significant concentration of ZO-1. For each white pixel in I_2, we determined its distance to the closest boundary point in I_1. In the resulting distance map shown in Figure 1E, the gray level varies inversely with distance value. The mean distance of ZO-1 from the nearest cell boundary was computed from the histograms of the distance values, normalized such that areas under the curves are equal. Less spread of ZO-1 from the cell boundary implies better tight-junction formation.

Electron microscopy

For scanning electron microscopy, 3.7% paraformaldehyde-fixed samples were rinsed in 1×PBS and then post-fixed with 1% osmium tetroxide for 1 h. Samples were

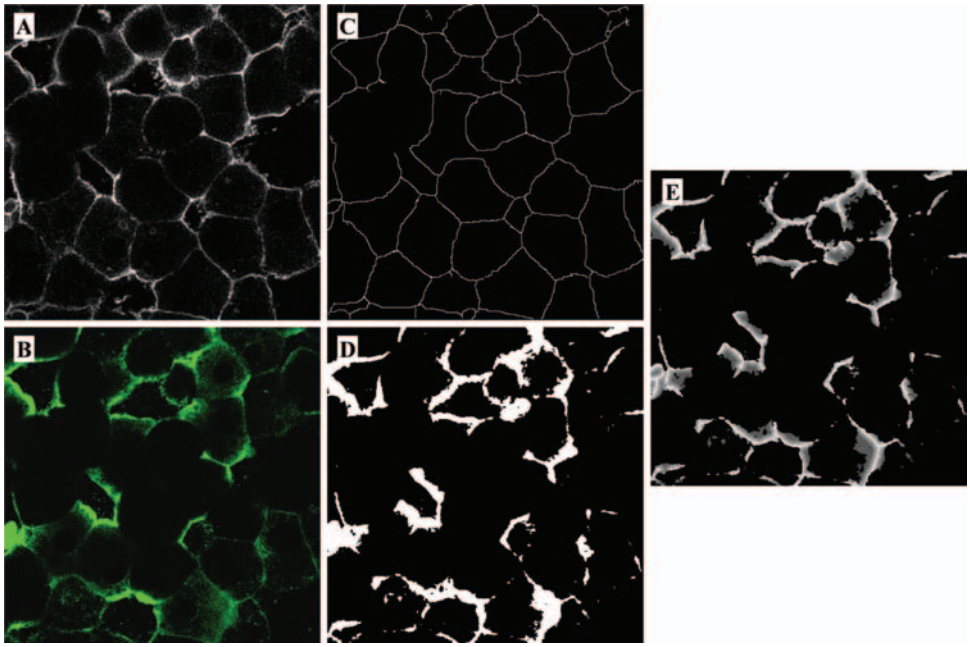

FIG. 1. Quantification of the spread of ZO-1 from the cell boundary. The gray component of the images of CD147-stained cells (**A**) was thresholded and subjected to a thinning algorithm to give 1-pixel-thick cell boundaries, image I_1 (**C**). The green component of the ZO-1-stained cells (**B**) was thresholded to give image I_2 (**D**). (**E**) Distance map of ZO-1 from cell boundary and the gray levels indicate distance from cell boundary. Less spread of ZO-1 from the cell boundary implies better tight-junctions formation. Color images available online at www.liebertpub.com/ten.

dehydrated using a graded series of ethanol (25%, 50%, 75%, 95%, and 100%). The samples were then critical-point-dried for 2 h in absolute alcohol, mounted onto a brass stub, and sputter-coated with platinum (JFC-1600, JEOL, Tokyo, Japan), before being viewed under a field emission scanning electron microscope (JSM-7400F, JEOL).

For transmission electron microscopy, samples were fixed in 2.5% glutaraldehyde for 2 h, postfixed with osmium tetroxide, dehydrated in ascending ethanol series and absolute acetone, and then embedded in araldite. Ultrathin sections were obtained using an ultramicrotome (Leica, Wetzlar, Germany), stained with lead citrate and observed under a transmission electron microscope (JEM-1010, JEOL).

Biliary excretion of fluorescein and rhodamine 123

For visualization of fluorescein excretion, 3 μg/mL fluorescein diacetate (Molecular Probes) in culture media was incubated with the cultures at 37°C for 45 min. The cultures were then rinsed and fixed before viewing under a confocal microscope (Fluoview 300) using a 40× water lens. Optical sectioning with a z resolution of 2 μm was used to obtain a 3D image stack of the sandwich culture.

For quantifying the biliary excretion of fluorescein and rhodamine 123, efflux studies based on the use of Ca^{2+} modulation to disrupt the tight junctions sealing the bile canaliculi were carried out.[12] Briefly stated, cultures were incubated in 30 μg/mL fluorescein diacetate or rhodamine 123 (Molecular Probes) in culture media at 37°C for 45 min. Subsequently, the incubation medium was removed and cultures were rinsed with Hanks' balanced salt solution (HBSS). Efflux was initiated by addition of 1.5 mL of Ca^{2+}-free buffer (5 mM EGTA [ethylene glycol-bis(β-aminoethyl-ether)-N,N,N′,N′-tetraacetate] in HBSS) or standard buffer (HBSS) to each dish. Aliquots of efflux buffer (0.25 mL) were removed at 2.5-min intervals within 10 min and analyzed using the microplate reader against respective fluorometric standards. The efflux of fluorescein and rhodamine 123 from the biliary canaliculi of hepatocytes was calculated by subtracting the area under the curve of efflux from cultures in standard buffer (nondisrupted tight junctions)

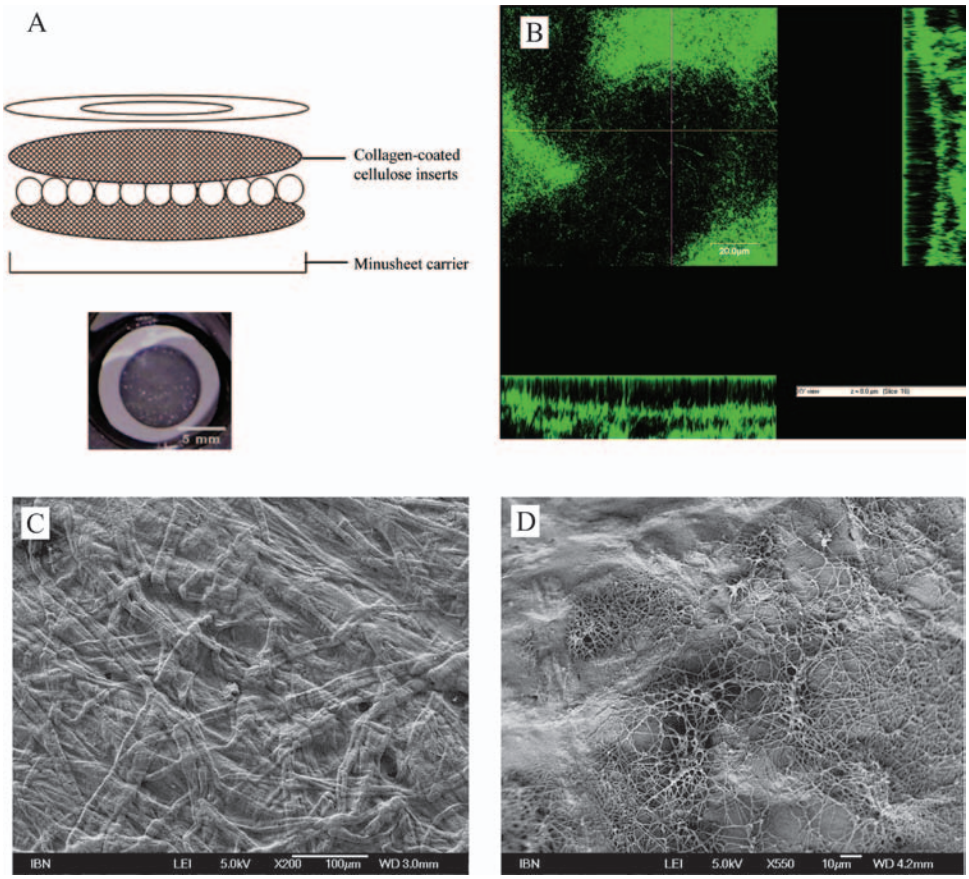

FIG. 2. Immediate presentation of 2 distinct matrix surfaces to primary hepatocytes in sandwich culture configuration. (**A**) Immediate collagen overlay culture configuration. (**B**) XYZ reconstruction of collagen coating on inserts using backscattering confocal microscopy. The 20-μm scale bar applies to the main XY image. The right and bottom panels in the same figure are the YZ and XZ cross-sections at the hairlines drawn on the main XY image, respectively. (**C**) Cellulose insert before collagen coating and (**D**) after collagen coating under scanning electron microscopy. Color images available online at www.liebertpub.com/ten.

from Ca^{2+}-free buffer (disrupted tight junctions) during the efflux period of 10 min.

Hepatocyte functional assays

All functional data were normalized to 10^6 cells based on the number of seeded cells. The daily albumin production was measured using the rat albumin enzyme-linked immunosorbent assay quantitation kit (Bethyl Laboratories Inc., Montgomery, TX). The urea production of the hepatocyte cultures incubated in culture medium with 2 mM ammonium chloride for 90 min was measured using the urea nitrogen kit (Stanbio Laboratory, Boerne, TX). The 7-ethoxyresorufin-O-deethylation assay, which is a measure of the deethylation activity of cytochrome P450 (CYP) 1A–associated monooxygenase enzymes, was initiated by incubating the cultures with 39.2 μM 7-ethoxyresorufin in culture medium at 37°C for 4 h. The amount of resorufin converted by the enzymes was calculated by measuring the resorufin fluorescence in the incubation medium at 543 nm (excitation)/570 nm (emission) against resorufin standards using the microplate reader (Tecan Trading AG).

Statistical methods

The Student *t*-test was used to analyze the statistical significance of the data. Values with a p value less than 0.05 were considered statistically significant.

Table 1. Diffusivity of Fluorescein Isothiocyanate-Dextrans of Various Molecular Weights across Collagen-Coated Cellulose Paper Inserts

Molecular weight (kDa)	*Diffusivity* $\times 10^8$ *(cm^2/s)*
9.5	1.49 ± 0.27
70	1.25 ± 0.27
150	1.11 ± 0.22

Values indicate diffusivity ± SD from 5 independent samples.

RESULTS

Characterization of immediate collagen overlay model

The immediate presentation of 2 distinct matrix surfaces to freshly plated primary hepatocytes without interference to their cell-cell interactions was achieved by sandwiching cells between 2 layers of gelled collagen-coated cellulose inserts (Fig. 2A). The 2 inserts were fastened by using Minusheet carriers, which also assisted in the easy handling of the collagen sandwich cultures. The fibrillar collagen gels formed a coating over as well as interdigitated with the cellulose inserts (Fig. 2B–D). The collagen coating over the inserts, which is important in presenting cell-matrix interaction surfaces, was, on average, 20.5 ± 1.7 μm

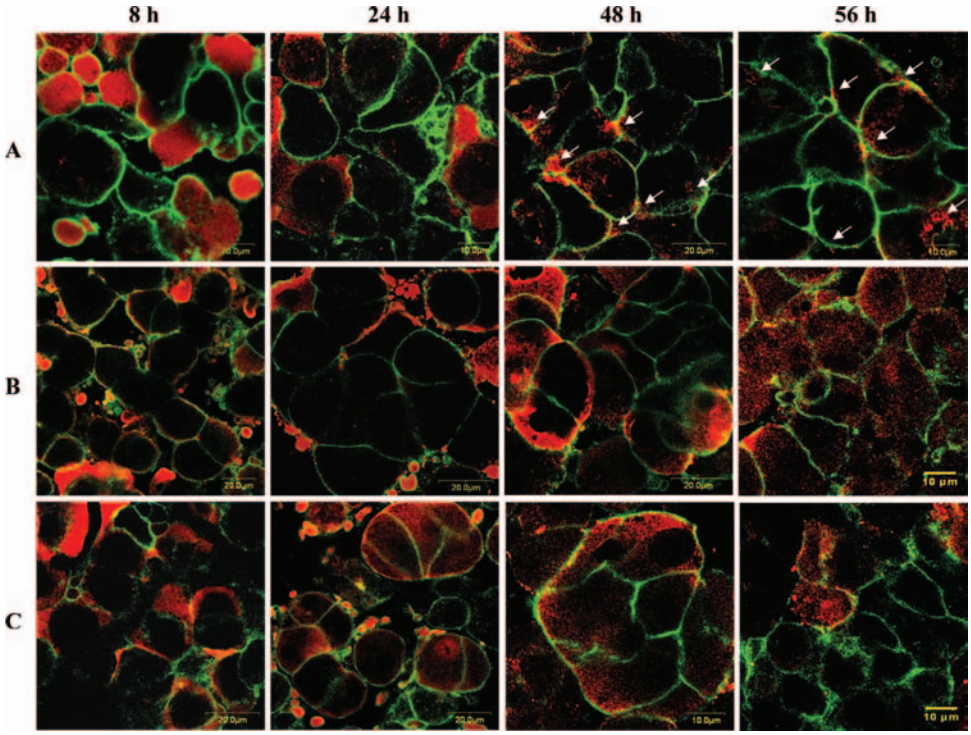

FIG. 3. Kinetics of formation of apical and basolateral domains by double-staining for apical multidrug resistance–associated protein (Mrp2) (*red*) and basolateral CD147 (*green*). (**A**) Immediate overlay. (**B**) 24-h overlay with insert. (**C**) Conventional 24-h overlay. Arrows point to Mrp2 concentrated in localized regions of cell-cell contacts. Color images available online at www.liebertpub.com/ten.

in thickness, measured under a confocal microscope (Fluoview 300). We investigated whether the cellulose inserts limited the mass transfer of molecules into the cell compartment. FITC-dextrans of various molecular weights of 9.5, 70, and 150 kDa (representative of a range of molecules of different sizes in the culture medium) displayed reasonable diffusivity of the order of 10^{-8} cm^2/s across the collagen-coated inserts (Table 1), similar to other porous membranes such as poly(ε-caprolactone) or collagen sheets.[21,22] The diffusivities of the FITC-dextrans showed an inverse trend toward their molecular weights, although only the difference between 9.5 and 70 kDa was statistically significant ($p < 0.05$). This indicated that the collagen-coated inserts did not show size discrimination and were freely permeable to molecules of various molecular weights in the culture medium.

Time point optimization for apicobasolateral formation between immediate and conventional 24-h overlay

We hypothesized that the immediate presentation of cell-matrix and cell-cell contacts as 2 polarity cues might enhance the formation of discrete apical and basolateral domains compared with the 24-h overlay controls, both with the collagen-coated insert and conventionally with liquid collagen followed by gelation. The kinetics of the formation of the apicobasolateral domains were studied by using the bile canalicular transporter, Mrp2, and the basolateral CD147 as apical and basolateral markers, respectively. While distinct basolateral localization of CD147 was observed within 8 h of culture for all the configurations, Mrp2 remained diffusively distributed over the cells at 8 h and 24 h. At 48 h and 56 h, the apical Mrp2 became concentrated in localized regions along cell-cell contacts (arrows, Fig. 3) for the immediate overlay, whereas the Mrp2 distribution for the 24-h overlay controls were more diffused. Since 48 h yielded the earliest significant differences in the apical repolarization of the hepatocytes in the different configurations, this time point was subsequently used to investigate potential differences in the cell-cell interactions between the cultured hepatocytes.

Immediate collagen overlay on cell morphology and cell-cell interactions

Scanning electron micrographs of hepatocytes at 48 h were used to help determine the effects of the immediate collagen overlay on cell morphology and cell-cell interactions. Figure 4 shows that cells cultured in the immediate overlay were more cuboidal in shape, were tightly organized, and featured cellular protrusions extending from one cell to another cell, whereas cells in the 24-h overlay controls were more rounded and generally more loosely interacting with other cells. In agreement with the electron micrograph observations, the tight junctional protein ZO-1 showed a more extensive localization at the cell boundary for the immediate overlay (Fig. 5A) as compared to the 24-h overlay controls (Fig. 5B and C), suggesting increased tight-junction interactions between cells in the immediate overlay. The mean distances of ZO-1 pixels from the nearest cell boundary in Figures 5A–C after normalization of the area under curve of the spread of ZO-1 from the cell boundary were 5, 15, and 14 pixels for the immediate overlay, 24-h overlay with insert, and liquid collagen, respectively. Transmission electron microscopy analysis also showed that hepatocytes in the immediate overlay reconstituted the bile canaliculus with typical microvilli and tight junctions on the surrounding plasma membrane (Fig. 5D). Overall, the results show that the immediate presentation of the collagen overlay facilitated lateral cell-cell interactions and the formation of tight junctions between cells.

Immediate collagen overlay on biliary excretion

Since tight junctions perform the function of a seal or fence to separate the bile canaliculus from the basolateral domains, we were interested in understanding how the improved tight junction formation in the immediate overlay at 48 h may influence the functional recovery of the 2 canalicular transporters important in xenobiotic efflux, namely, Mrp2 and P-gp. The functional activity of Mrp2 was evaluated by examining the localization of fluorescein, a high-affinity Mrp2 substrate, by incubation with the nonfluorescent precursor, fluorescein diacetate. The latter enters the cell by passive diffusion, where it is hydrolyzed

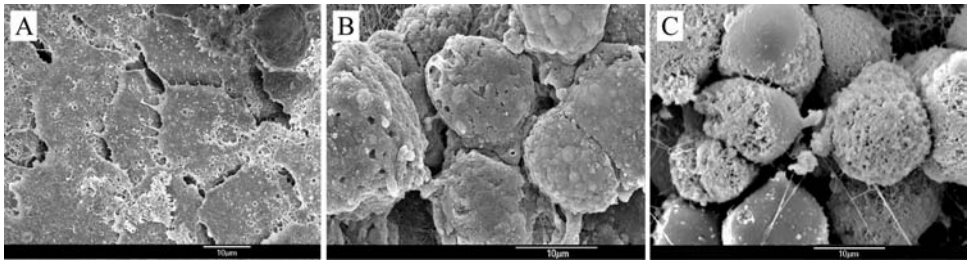

FIG. 4. Scanning electron micrographs of cell morphology at 48 h of culture. (**A**) Immediate overlay. (**B**) 24-h overlay with insert. (**C**) Conventional 24-h overlay.

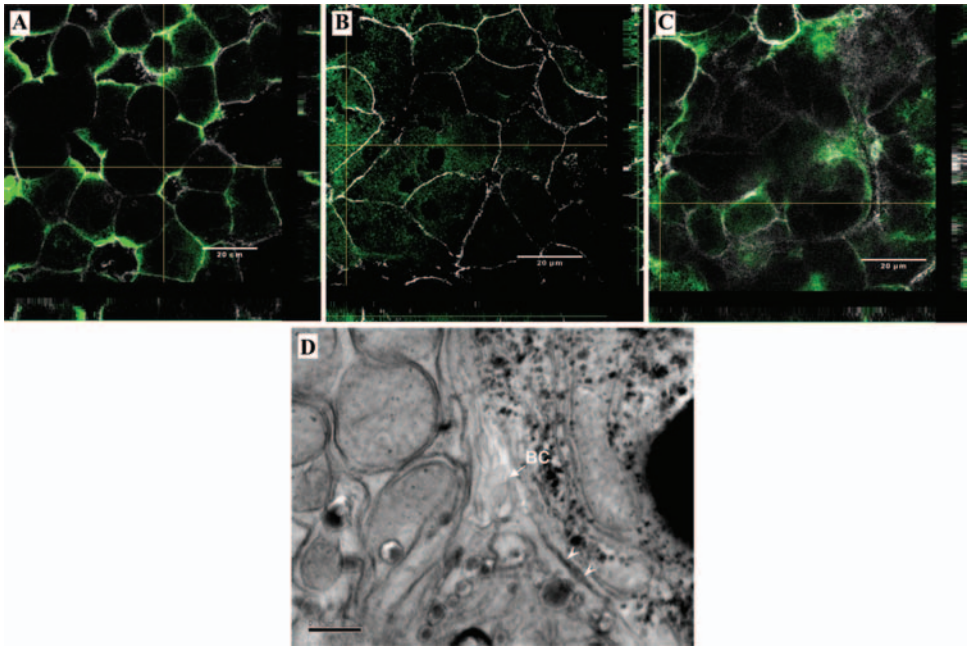

FIG. 5. Formation of tight junctions at 48 h of culture. (**A–C**) XYZ reconstruction of ZO-1 (green) counterstained with basolateral CD147 (gray). (**A**) Immediate overlay. (**B**) 24-h overlay with insert. (**C**) Conventional 24-h overlay. (**D**) Transmission electron micrograph of the cell boundary hepatocytes in immediate overlay cultured for 48 h. Typical microvilli in the biliary canaliculi (*BC*) and tight junctions on the surrounding plasma membrane *(arrowheads)* can be observed. Scale bar refers to 0.5 μm. Color images available online at www.liebertpub.com/ten.

by intracellular esterases into fluorescein before it is excreted by Mrp2.[23] At 24 h of culture, fluorescein was concentrated in the intracellular space for all the configurations (Fig. 6, left column). At 48 h of culture, fluorescein began to show a more concentrated localization in the space between hepatocytes (arrows, Fig. 6, middle column) for the immediate overlay, which indicated that fluorescein was being excreted into the apical domain of the cells, in contrast to the significant intracellular retention of fluorescein in the 24-h overlay controls. The amount of fluorescein excreted was increased for all the configurations at 72 h of culture as compared to earlier time points, but the fluorescein excretion was clearly the most extensive for the immediate overlay configuration (Fig. 6, right column). To quantify the functional activity of Mrp2 and P-gp, the efflux of their respective model substrates, fluorescein and rhodamine 123, from the apical domain or bile canaliculi was measured by the use of Ca^{2+} modulation to disrupt tight junctions fencing the bile canaliculi.[12] Rhodamine 123, unlike fluorescein diacetate, is taken up at the basolateral membrane via an active Oatp1a4-mediated process and is excreted at the canalicular membrane by P-gp.[24] The efflux of fluorescein and rhodamine 123 from cultures in Ca^{2+}-free buffer (5 mM EGTA in HBSS) and standard buffer (HBSS) was measured over 10 min. The efflux of the substrates from the bile canaliculi was calculated by subtracting the area under efflux curve of cultures in standard buffer (nondisrupted tight junctions) from Ca^{2+}-free buffer (disrupted tight junctions) during the efflux period of 10 min. Table 2 shows that the efflux of fluorescein and rhodamine 123 from hepatocyte bile canaliculi at 48 h of culture were statistically significantly higher for the immediate overlay compared with the 24-h overlay controls ($p < 0.05$). This finding signified an improved functional recovery of the excretory activity of Mrp2 and P-gp. Since the active transport of the canalicular transporters constitutes the major route of waste elimination from the cell,[13] improved functional recovery of the transporters may lead to more efficient excretion of waste products from the cell. This, in turn, may benefit their functional maintenance.

Immediate collagen overlay on hepatocyte functional maintenance

We hypothesized that the improved excretory function of hepatocytes presented with the immediate overlay may promote the maintenance of other liver-specific functions of hepatocytes, such as their synthetic, detoxifying, and metabolic activities. Figure 7 shows that the albumin secretion, urea production, and normalized 7-ethoxyresorufin-O-deethylation cytochrome P450 activity (relative to freshly isolated hepatocytes) of hepatocytes cultured with the immediate overlay were significantly higher than those of the 24-h overlay controls over 15 days of culture ($p < 0.05$). The functional enhancement was greatest within the first 3–5 days, which was translated into a higher level of functions

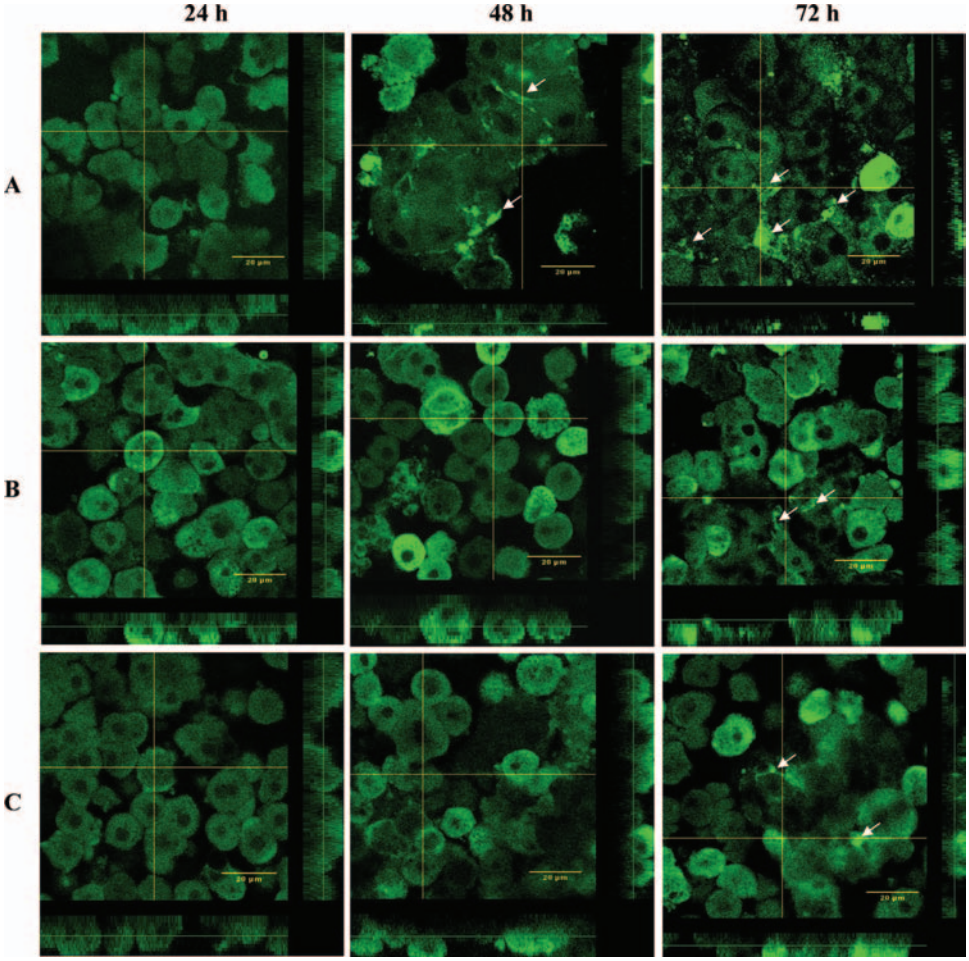

FIG. 6. Functional polarity at 48 h of culture. XYZ reconstruction of the localization of fluorescein in hepatocyte cultures over time. (**A**) Immediate overlay. (**B**) 24-h overlay with insert. (**C**) Conventional 24-h overlay. Arrows point to fluorescein concentrated in the space between hepatocytes. Color images available online at www.liebertpub.com/ten.

upon stabilization. The coincident improvement in the functional recovery of canalicular transporters and the functional maintenance of hepatocytes at early points of culture may indicate that improving the excretory function of hepatocytes is a valuable strategy to improve the functional maintenance of hepatocytes over a longer culture period.

DISCUSSION

The excretory function of hepatocytes is a major function of the liver, which plays an important role in the elimination of metabolites and toxins from the body.[25] In the liver, the excretion of a variety of endogenous and exogenous materials from the cell into the bile canaliculi is an active process mediated by a variety of adenosine triphosphate–dependent efflux pumps on the canalicular membrane.[13] Tissue-engineered liver constructs based on primary hepatocytes possess limited excretory function in comparison to the native liver because of the endocytosis of the canalicular transporters after isolation with collagenase.[12,26] Studies have shown that alterations in the expression or localization of canalicular transporters such as the bilirubin pump, Mrp2, can lead to altered function.[12,27,28] The presentation of extrinsic cues to the cells may be required for the cells to re-establish polarity *in vitro* so as to facilitate the relocation of the transporters to the canalicular membrane, which can take place over time in culture.[29,30] Little is known about the signals and molecules involved in generating cell polarity in hepatocytes, although these have been extensively studied in columnar epithelial models such as MDCK.[16,31,32] Hepatic polarity is structurally dissimilar from columnar polarity that has a single apical and a single basal surface, and is characterized instead by an apical (bile canalicular) pole that divides 2 basolateral (sinusoidal) surfaces in contact with the matrix.[33,34] Insights from columnar epithelia may shed light on the importance of cell-matrix and cell-cell contacts in the generation of cell polarity.[16,17,31,32] Yeaman *et al.* proposed that distinct

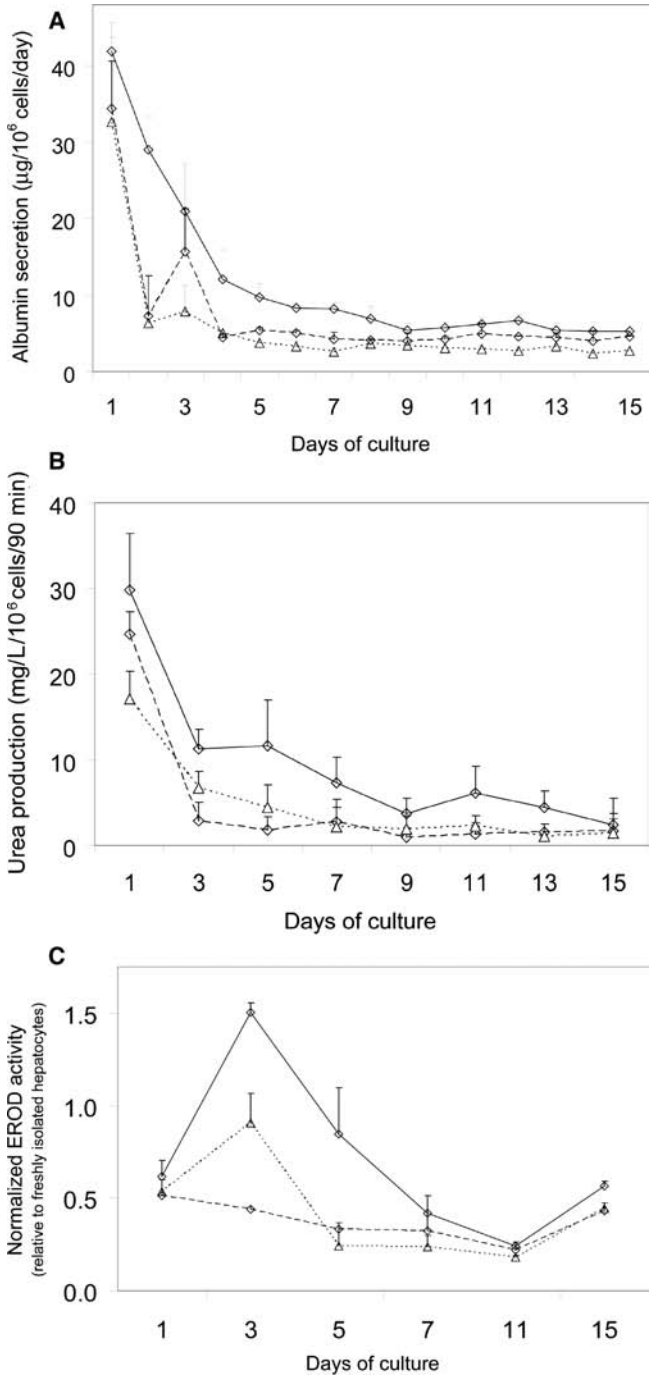

FIG. 7. Functional maintenance of hepatocytes. (**A**) Albumin secretion. (**B**) Urea production. (**C**) Normalized 7-ethoxyresorufin-O-deethylase cytochrome P450 activity relative to freshly isolated hepatocytes. Solid line: immediate overlay; dashed line: 24-h overlay with insert; dotted line: conventional 24-h overlay.

cell-matrix and cell-cell contacts are required to orientate the apicobasolateral axis of polarity relative to the extrinsic cues and to initiate cytoskeletal reorganization and signaling complexes at the contacting membranes.[18] On the basis of this model, the success of the sandwich culture in promoting hepatocyte repolarization may lie in the presentation of a second discrete matrix surface upon collagen overlay after 24 h, during which cells are allowed to form intercellular contacts. The importance of distinct cell-matrix and cell-cell contacts in polarity generation may point to why earlier work by Chandra *et al*. reported no enhancement in hepatocyte repolarization when they used ungelled collagen to overlay hepatocytes 1 h after seeding.[35] Overlaying hepatocytes with ungelled collagen before they have formed tight cell-cell interactions probably interfered with the formation of discrete plasma membrane contacts of both types (cell-matrix and cell-cell) crucial to cell repolarization. Our data show that the immediate and discrete presentation of the collagen and cell-cell contacts (temporal and spatial presentation of polarity cues) may be important in the repolarization of primary hepatocytes (Figs. 3 and 6), which may facilitate the functional recovery of canalicular transporters (Table 2) important in xenobiotic efflux.

TABLE 2. EFFLUX OF FLUORESCEIN AND RHODAMINE 123 FROM THE BILE CANALICULI OF HEPATOCYTES OVER 10 MINUTES FOR IMMEDIATE AND 24-H OVERLAY SANDWICH CULTURES AT 48 H OF CULTURE

	Efflux from bile canaliculi (μg/mL per 10^6 cells)	
	Fluorescein	*Rhodamine 123*
Immediate overlay	0.62 ± 0.07	4.68 ± 1.12
24-h overlay with insert	0	0.06 ± 0.11
Conventional 24-h overlay	0	1.33 ± 1.25

Values indicate efflux (μg/mL) ± SE from 3 independent experiments.

An improvement in the biliary excretion of cultured hepatocytes may also be favorable for their overall functional maintenance. This relationship has been implicated in "gold standard" hepatocyte culture models such as spheroids,[4,5] sandwich cultures,[6,7] and co-cultures[8] that consistently share similar traits of improved biliary formation, together with high levels of differentiated functions. We also found that the early recovery of the excretory functions of Mrp2 and P-gp (Table 2) was coupled to an enhancement in the maintenance of the albumin secretion and detoxification functions of the cultured hepatocytes, which were coincidentally greatest within the first few days of culture (Fig. 7). More important, the early functional enhancement was translated into a higher level of long-term functions that was also reported in improved culture models such as spheroid and sandwich cultures.[33,36] Therefore, improving the repolarization and excretory function of hepatocytes may be an important strategy to improve the functional maintenance of hepatocytes over a longer culture period. Supplementation to the culture media might also intensify the long-term differentiation effects of various culture conditions. A previous study showed that the increase in albumin secretion of hepatocytes in sandwich system after 1 week of culture was positively correlated to the level of hydrocortisone supplement in serum-free

media, and addition of 75 ng/mL hydrocortisone was required for the albumin secretion to increase over time.[33] In our system, a 10-fold increase in dexamethasone concentration (from 39 to 390 ng/mL) can also cause the albumin secretion to elevate (data not shown). Further work will investigate the coordinated effects of soluble factors such as retinoic acid[37] and extracellular polarity cues on the repolarization and differentiation of hepatocytes.

This work represents a systematic approach toward improving the excretory function of primary hepatocytes by the incorporation of extracellular polarity cues based on our fundamental understanding of epithelial cell repolarization. The immediate presentation of the collagen matrix overlay was shown to enhance repolarization, the functional activity of canalicular transporters Mrp2 and P-gp, and the functional maintenance of primary hepatocytes over 2 weeks of culture. The improvement in the excretory function of hepatocytes for the removal of waste products deleterious to cells may improve the functional maintenance and the *in vivo* fidelity of tissue-engineered liver constructs.

ACKNOWLEDGMENTS

We acknowledge the financial and infrastructure support from the Institute of Bioengineering and Nanotechnology, and Biomedical Research Council (BMRC) of the Agency for Science, Technology and Research (A*STAR), and the National University of Singapore (NUS). We are grateful for the invaluable scientific inputs of Dr. Chia Ser Mien and Dr. Karl Schumacher. We thank members of the Yu laboratory, especially the Microliver Tissue Group and the Electron Microscopy Unit (NUS), for their technical and scientific assistance with the work.

REFERENCES

1. Riordan, S.M., and Williams, R. Acute liver failure: targeted artificial and hepatocyte-based support of liver regeneration and reversal of multiorgan failure. J. Hepatol. **32**, 63, 2000.
2. Allen, J.W., and Bhatia, S.N. Engineering liver therapies for the future. Tissue Eng. **8**, 725, 2002.
3. Ostapowicz, G., Fontana, R.J., Schiodt, F.V., Larson, A., Davern, T.J., Han, S.H., McCashland, T.M., Shakil, A.O., Hay, J.E., Hynan, L., Crippin, J.S., Blei, A.T., Samuel, G., Reisch, J., and Lee, W.M.; U.S. Acute Liver Failure Study Group. Results of a prospective study of acute liver failure at 17 tertiary care centers in the United States. Ann. Intern. Med. **137**, 947, 2002.
4. Abu-Absi, S.F., Friend, J.R., Hansen, L.K., and Hu, W.S. Structural polarity and functional bile canaliculi in rat hepatocyte spheroids. Exp. Cell Res. **274**, 56, 2002.
5. Depreter, M., Walker, T., De Smet, K., Beken, S., Kerckaert, I., Rogiers, V., and Roels, F. Hepatocyte polarity and the peroxisomal compartment: a comparative study. Histochem. J. **34**, 139, 2002.
6. LeCluyse, E.L., Audus, K.L., and Hochman, J.H. Formation of extensive canalicular networks by rat hepatocytes cultured in collagen-sandwich configuration. Am. J. Physiol. **266**, C1764, 1994.
7. Liu, X., Chism, J.P., LeCluyse, E.L., Brouwer, K.R., and Brouwer, K.L.R. Correlation of biliary excretion in sandwich-cultured rat hepatocytes and in vivo in rats. Drug Metab. Dispos. **27**, 637, 1999.
8. Bhandari, R.N., Riccalton, L.A., Lewis, A.L., Fry, J.R., Hammond, A.H., Tendler, S.J., and Shakesheff, K.M. Liver tissue engineering: a role for co-culture systems in modifying hepatocyte function and viability. Tissue Eng. **7**, 345, 2001.
9. Bissell, D.M., Caron, J.M., Babiss, L.E., and Friedman, J.M. Transcriptional regulation of the albumin gene in cultured rat hepatocytes. Role of basement–membrane matrix. Mol. Biol. Med. **7**, 187, 1990.
10. Mikos, A.G., Thorsen, A.J., Czerwonka, L.A., Bao, Y., Winslow, D.N., Vacanti, J.P., and Langer, R. Preparation and characterization of poly(L-lactic acid) foams. Polymer **35**, 1068, 1994.
11. Sudo, R., Ikeda, S., Sugimoto, S., Harada, K., Hirata, K., Tanishita, K., Mochizuki, Y., and Mitaka, T. Bile canalicular formation in hepatic organoid reconstructed by rat small hepatocytes and nonparenchymal cells. J. Cell. Physiol. **199**, 252, 2004.
12. Liu, X., LeCluyse, E.L., Brouwer, K.R., Gan, L.S., Lemasters, J.J., Stieger, B., Meier, P.J., and Brouwer, K.L. Biliary excretion in primary rat hepatocytes cultured in a collagen-sandwich configuration. Am. J. Physiol. **277**, G12, 1999.
13. LeBlanc, G.A. Hepatic vectorial transport of xenobiotics. Chem. Bio. Interact. **90**, 101, 1994.
14 Suzuki, T., Nishio, K., and Tanabe, S. The MRP family and anticancer drug metabolism. Curr. Drug Metab. **2**, 367, 2001.
15. Hoffmaster, K.A., Turncliff, R.Z., LeCluyse, E.L., Kim, R.B., Meier, P.J., and Brouwer, K.L.R. P-glycoprotein expression, localization, and function in sandwich-cultured primary rat and human hepatocytes: relevance to the hepatobiliary disposition of a model opioid peptide. Pharm. Res. **21**, 1294, 2004.
16. Wang, A.Z., Ojakian, G.K., and Nelson, W.J. Steps in the morphogenesis of a polarized epithelium. I. Uncoupling the roles of cell–cell and cell–substratum contact in establishing plasma membrane polarity in multicellular epithelial (MDCK) cysts. J. Cell Sci. **95**, 137, 1990.
17. Gudjonsson, T., Ronnov-Jessen, L., Villadsen, R., Rank, F., Bissell, M.J., and Petersen, O.W. Normal and tumor-derived myoepithelial cells differ in their ability to interact with luminal breast epithelial cells for polarity and basement membrane deposition. J. Cell Sci. **115,** 39, 2002.
18. Yeaman, C., Grindstaff, K.K., and Nelson, W.J. New perspectives on mechanisms involved in generating epithelial cell polarity. Physiol. Rev. **79**, 79, 1999.
19. Dong, L.C., Hoffman, A.S., and Yan, Q. Dextran permeation through poly(N-isopropylacrylamide) hydrogels. J. Biomater. Sci. Polym. Ed. **5**, 473, 1994.
20. Seglen, P.O. Preparation of isolated rat liver cells. Methods Cell Biol. **13**, 29, 1976.
21. Lin, W.J., and Lu, C.H. Characterization and permeation of microporous poly(ε-caprolactone) films. J. Membrane Sci. **198**, 109, 2002.

22. Vernon, R.B., Gooden, M.D., Lara, S.L., and Wight, T.N. Native fibrillar collagen membranes of micron-scale and submicron thicknesses for cell support and perfusion. Biomaterials **26**, 1109, 2005.
23. Zamek-Gliszczynski, M.J., Xiong, H., Patel, N.J., Turncliff, R.Z., Pollack, G.M., and Brouwer, K.L. Pharmacokinetics of 5 (and 6)-carboxy-2′,7′-dichlorofluorescein and its diacetate promoiety in the liver. J. Pharmacol. Exp. Ther. **304**, 801, 2003.
24. Annaert, P.P., and Brouwer, K.L. Assessment of drug interactions in hepatobiliary transport using rhodamine 123 in sandwich-cultured rat hepatocytes. Drug Metab. Dispos. **33**, 388, 2005.
25. van Montfoort, J.E., Hagenbuch, B., Groothuis, G.M., Koepsell, H., Meier, P.J., and Meijer, D.K. Drug uptake systems in liver and kidney. Curr Drug Metab. **4**, 185, 2003.
26. Graf, J., and Boyer, J.L. The use of isolated rat hepatocyte couplets in hepatobiliary physiology. J. Hepatol. **10**, 387, 1990.
27. Kojima, H., Nies, A.T., Konig, J., Hagmann, W., Spring, H., Uemura, M., Fukui, H., and Keppler, D. Changes in the expression and localization of hepatocellular transporters and radixin in primary biliary cirrhosis. J. Hepatol. **39**, 693, 2003.
28. Kikuchi, S., Hata, M., Fukumoto, K., Yamane, Y., Matsui, T., Tamura, A., Yonemura, S., Yamagishi, H., Keppler, D., and Tsukita, S. Radixin deficiency causes conjugated hyperbilirubinemia with loss of Mrp2 from bile canalicular membranes. Nat. Genet. **31**, 320, 2002.
29. Zhang, P., Chandra, P., Kramarcy, N., and Brouwer, K.R. Time course of multidrug resistance-associated protein (Mrp) 2 expression, localization and function in sandwich-cultured rat hepatocytes (SCRH) (Abstract). AAPS Pharm. Sci. **3**, 1522, 2001.
30. Hoffmaster, K.A., Turncliff, R.Z., LeCluyse, E.L., Kim, R.B., Meier, P.J., and Brouwer, K.L. P-glycoprotein expression, localization, and function in sandwich-cultured primary rat and human hepatocytes: relevance to the hepatobiliary disposition of a model opioid peptide. Pharm. Res. **21**, 1294, 2004.
31. Vega-Salas, D.E., Salas, P.J., Gundersen, D., and Rodriguez-Boulan, E. Formation of the apical pole of epithelial (Madin–Darby canine kidney) cells: polarity of an apical protein is independent of tight junctions while segregation of a basolateral marker requires cell–cell interactions. J. Cell Biol. **104**, 905, 1987.
32. Ojakian, G.K., Nelson, W.J., and Beck, K.A. Mechanisms for de novo biogenesis of an apical membrane compartment in groups of simple epithelial cells surrounded by extracellular matrix. J. Cell Sci. **110**, 2781, 1997.
33. Dunn, J.C., Tompkins, R.G., and Yarmush, M.L. Long-term *in vitro* function of adult hepatocytes in a collagen sandwich configuration. Biotechnol. Prog. **7**, 237, 1991.
34. Zegers, M.M., and Hoekstra, D. Mechanisms and functional features of polarized membrane traffic in epithelial and hepatic cells. Biochem. J. **336**, 257, 1998.
35. Chandra, P., Lecluyse, E.L., and Brouwer, K.L. Optimization of culture conditions for determining hepatobiliary disposition of taurocholate in sandwich-cultured rat hepatocytes. In Vitro Cell Dev. Biol. Anim. **37**, 380, 2001.
36. Tong, J.Z., De Lagausie, P., Furlan, V., Cresteil, T., Bernard, O., and Alvarez, F. Long-term culture of adult rat hepatocyte spheroids. Exp. Cell Res. **200**, 326, 1992.
37. Falasca, L., Favale, A., Serafino, A., Ara, C., and Conti Devirgiliis, L. The effect of retinoic acid on the re-establishment of differentiated hepatocyte phenotype in primary culture. Cell Tissue Res. **293**, 337, 1998.

Address reprint requests to:
Hanry Yu, Ph.D.
Institute of Bioengineering and Nanotechnology
*A*STAR*
Singapore

Email: phsyuh@nus.edu.sg